https://doi.org/10.1016/j.precisioneng.2017.08.010

Precision machining of 'water-drop' surface by single point diamond grinding

Quanli Zhang[1,2,3], Qingliang Zhao[2*], Suet To[3], Bing Guo[2] and Zhimin Rao[2]

[1] *College of Mechanical and Electrical Engineering, Nanjing University of Aeronautics and Astronautics, Nanjing, 210016, China*

[2] Center for Precision Engineering, School of Mechatronics Engineering, Harbin Institute of Technology, Harbin, 150001, China

[3] State Key Laboratory of Ultra-precision Machining Technology, The Hong Kong Polytechnic University, Hong Kong

*Corresponding Author / E-mail: zhangql606@163.com, TEL: +86-025-84895857, FAX: +86-025-84895857

zhaoqingliang@hit.edu.cn, TEL: +86-451 8640 2683, FAX: +86-451 8641 5244

Abstract

With good prospect for machining functional surfaces on hard and brittle materials, single point diamond grinding (SPDG) has been applied, but its wider application still need more effort and development. In the present work, an appropriate dressing method is firstly proposed to obtain a sharp edge on a fine grit diamond wheel. With the prepared wheel, a designed 'water-drop' surface is machined by single point diamond grinding (SPDG), with the integration of the rotary *B* axis. Based on the proposed compensation method, the form accuracy and surface finish of the machined functional surface reaches 0.64 μm (*PV*), 6 nm (S_a) for the Φ20 mm 'water-drop' surface on binderless tungsten carbide.

Keywords: Single point diamond grinding; 'water-drop' surface; wheel wear; compensation

1. Introduction

With the continuously increasing requirements for more and more optical elements, hard and brittle materials are gradually replacing the traditional molds made of steel, aluminum, and copper materials. For example, tungsten carbide (WC) is widely used in the fabrication of molds to meet the requirement of high volume production for glass molding. Compared with conventional materials, these materials provide with high strength, high hardness, and great chemical and corrosion resistance at elevated temperature. In addition, to meet the requirement of miniaturization and integration, various types of functional surface, such as rotational symmetrical on or off the axis surface, lens arrays and freeform surfaces, have been machined by ultra-precision diamond turning and milling [1]. However, they are not suitable for machining hard and brittle materials due to the serious tool wear caused by the mechanical and chemical aspects at high temperature and pressure [2].

Fortunately, ultra-precision grinding can be utilized to machine hard and brittle materials to meet the requirements of high form accuracy and surface smoothness [3]. Parallel grinding methodology has been widely utilized to machine functional surfaces on such materials [4, 5], such as spherical, aspherical and Fresnel surfaces. As a good candidate for machining functional surfaces on hard and brittle materials, the recently developed grinding methodology, wheel normal grinding or single point diamond grinding, has been studied and utilized [4, 6-10]. In this grinding process, to solve the problem of size limitation for the machined surface [11], a sharp edge on the diamond wheel is necessary to prevent interference between the diamond wheel and the designed

surface [12, 13].

However, during ultra-precision grinding, diamond wheel wear and various error sources result in form deviation and worsened surface finish of the machined surface [14-17]. Especially for single point diamond grinding of structural surfaces, the sharp edge on the diamond wheel is of great importance and the rapid wear always makes it more difficult to achieve the designed surface profile [17]. Therefore, the right choice and dressing of a diamond wheel is the first prerequisite for ultra-precision grinding. Even during the machining process, the on-machine dressing of the wheel is needed if obvious wheel wear appears. In addition, the compensation of tool path based on the on-machine measurement needs to be performed to obtain better form accuracy [18-20].

This work reports investigations on single point diamond grinding of a designed 'water-drop' surface. Firstly, the dressing method of the diamond wheel to obtain a sharp edge is proposed and the wheel wear mechanism is explored. Then, grinding of the designed 'water-drop' surface on binderless WC is performed with the linkage movement of the *X, Z* and *B* axes. Finally, error compensation is undertaken, focusing on the alleviation of the center dent error.

2. Designed 'water-drop' surface and the grinding methodology

Fig. 1 shows the cross sectional profile and 3D surface of the designed 'water-drop' surface. To prevent the interference between the Φ16 mm diamond wheel and the workpiece, the cross-sectional profile was designed according to Eqs.(1) to (3):

$$z_1 = 0.05 \cdot e^{-0.1x} \tag{1}$$

$$z_2 = \cos(\frac{4\pi \cdot x}{10}) \tag{2}$$

$$z = z_1 \cdot z_2 = 0.05 \cdot e^{-0.1 \cdot x} \cdot \cos\left(\frac{4\pi \cdot x}{10}\right) \tag{3}$$

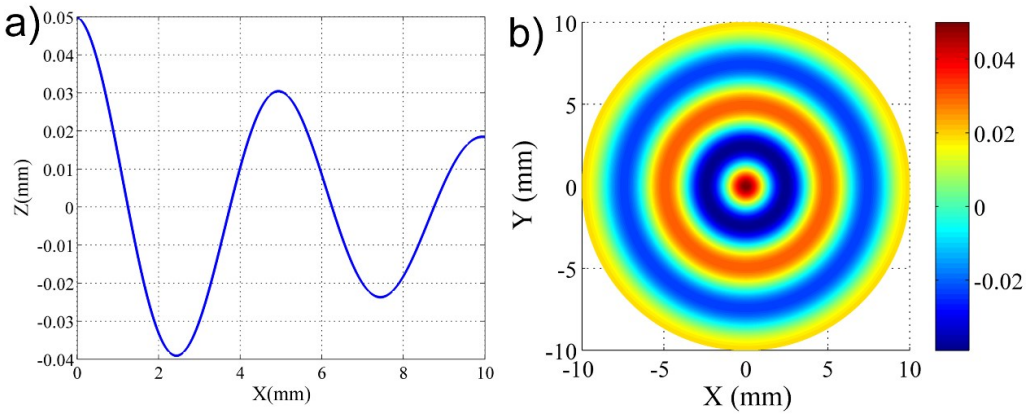

Fig. 1 (a) Cross-sectional profile; (b) the 3D surface of the designed "water-drop" surface (plotted by a MATLAB program)

Single point grinding is a newly developed grinding methodology, which is more appropriate to machine structural surfaces. At a higher grinding spindle speed and with finer grinding parameters, the contact area between the diamond wheel and the machined workpiece surface can be seen as constant, which is similar to the single point diamond turning (SPDT). In the present study, a fine grits diamond wheel with a sharp edge is applied to machine the designed 'water-drop' surface by single point diamond grinding. The grinding process is conducted in a parallel mode by the linkage movement of the *X* and *Z* axes, with the diamond wheel fed from the side of the part to the center along *X* axis. To ensure that the sharp edge of the diamond wheel participates in the material removal and surface generation process, the diamond wheel is moved with a gradient tilted angle by integrating *B* axis rotation to adjust the relative position of the diamond wheel and workpiece surface, as illustrated in Fig. 2.

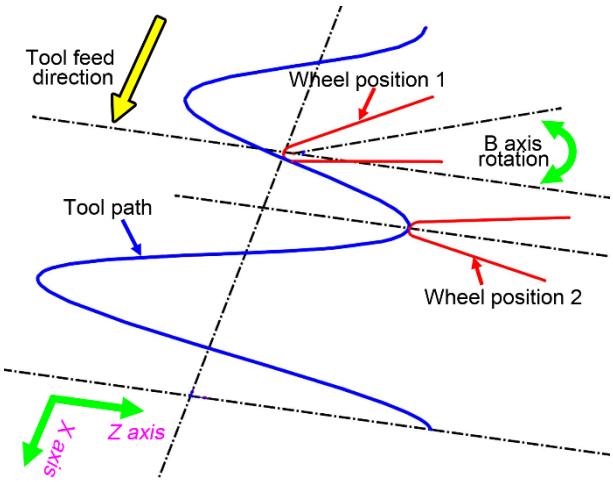

Fig. 2 Illustration of the grinding methodology

To ensure the grinding efficiency and the quality of the machined surface (both surface roughness and form accuracy), the grinding process is divided into three stages: rough grinding, fine grinding and ultra-fine grinding. The flow chart of the grinding process is shown in Fig. 3. Furthermore, the on-machine measurement and tool path compensation are performed to obtain better form accuracy. Specifically, compensation of the tool path is undertaken with the obtained error data by the on-machine LVDT probe, and a new tool path is generated accordingly.

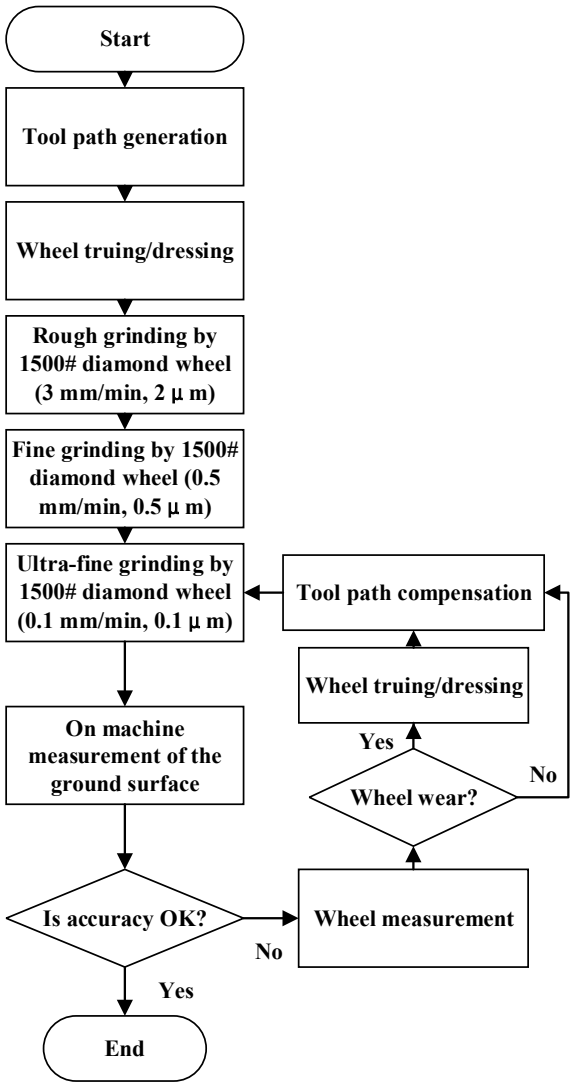

Fig. 3 A flow chart to illustrate the grinding protocol of 'water-drop' surface

3. Experiments

3.1 Materials and machining

Commercially available binderless WC of 22 mm in diameter (DIJET INDUSTRIAL CO., LTD) was machined on an ultra-precision machine (Moore Nanotech 450UPL, USA), equipped with an on-machine measuring probe. Photographs of the grinding setup are shown in Fig. 4. The detailed properties of the binderless WC is listed in Table 1. In this study, a resin bonded diamond wheel of 1500# grit size and 16 mm in diameter with a carbide mandrel (Diagrind, Inc., USA) was chosen for

grinding. The ratio of the volume of the diamond grits to the volume of bond in the grinding wheel is 100%, and the wheel was fabricated with a 60°sharp edge.

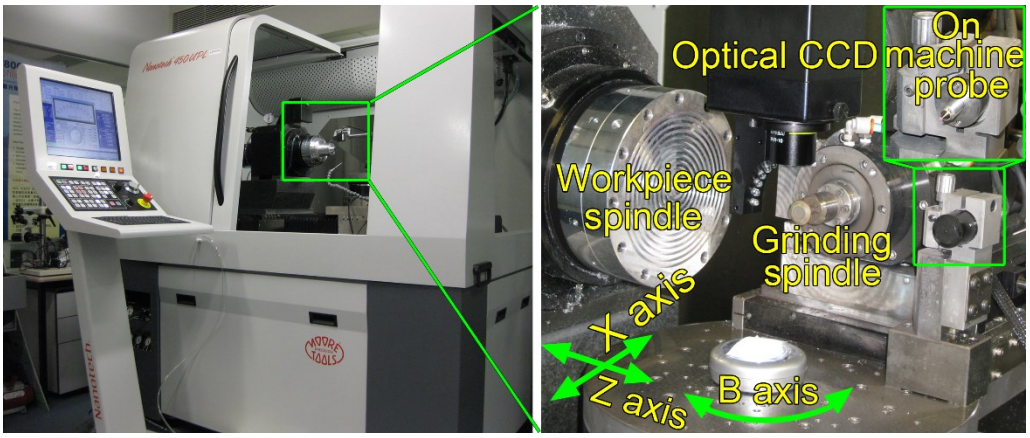

Fig. 4 Photographs of the grinding setup

Table 1 Mechanical properties of binderless WC material

Elastic modulus E (GPa)	680
Vikers hardness H (GPa)	26.37
Fracture toughness K_{IC} (MPa $m^{1/2}$)	5.292
Density ρ (g/cm^3)	15.5
Size of workpiece (mm)	Φ22×5

3.2 Characterization and measurement

A 3D optical measuring system (Alicona IFM G4) was used to examine the profile of the diamond wheel after grinding, and a scanning electron microscope (SEM, Hitachi TM3000) was applied to identify the worn mechanism of the diamond wheel. The surface roughness and the cross-sectional profile of the machined ‘water-drop’ surface was measured and analyzed by a Nexview 3D profiler (ZygoLamda) and an atomic force microscope (Park's XE-70). In addition, an on-machine LVDT probe and optical CCD were utilized to measure the form accuracy of the ground surface and to examine the macro wheel wear, respectively.

4. Results and discussion

4.1 Diamond wheel wear and dressing

In the ultra-precision grinding process, the wear of the diamond wheel results in a dulling of the abrasive grits and a size deviation of the wheel, which reduces the grinding efficiency and has a great impact on the surface integrity and form accuracy of the workpiece [15, 21]. Therefore, corresponding conditioning of the wheel is essential. “Grinding is dressing” is a well-known slogan in the grinding field [15], which indicates the extreme importance of dressing the wheels before and during the grinding process. Therefore, to find an appropriate method to align and dress the diamond wheel effectively is the primary task before the machining of the structural surface [12, 13, 22]. In addition, the wear mechanism needs to be explored.

Table 2 Detail dressing parameters for the 1500# diamond wheel

Dressing	Diamond nib/Al_2O_3 stick	
	Feed rate (mm/min)	0.5
	Depth of dressing (μm/pass)	5
	Truer (rpm)	300
	Wheel (rpm)	2,000
Coolant	CLAIRSOL 350	MQL

In this work, to achieve a sharp edge on the 1500# diamond wheel, a diamond nib was firstly used to true it, and then an Al_2O_3 stick was applied to dress the edge to obtain an arc shape and make the abrasive grits protrude above the resin bond, as illustrated in Fig. 5. The diamond nib is of a cone shape with a 60° apex angle. The face of the cubic Al_2O_3 stick is in a size of 13×13 mm. After a series of wheel dressing experiments, a spherical surface of 8 mm in radius formed in the face.

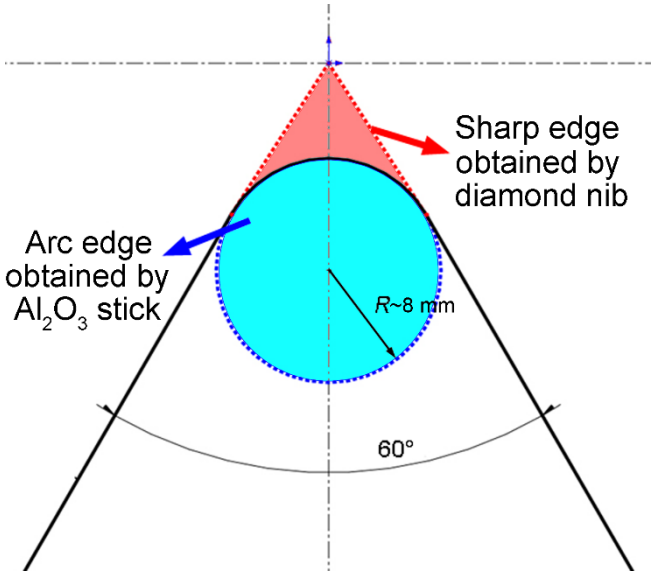

Fig. 5 Illustration of the truing and dressing schematic diagram

The detail wheel truing/dressing parameters are listed in Table 2, and the setup is shown in Fig. 6. Firstly, the choice of the truing and dressing depth is a critical factor that determines whether the required shape of the diamond wheel could be achieved. It was found that when the dressing depth was less than 1/2 the average size of the diamond grits, the diamond nib was ground by the wheel, and the wheel could not be trued effectively. With the gradual increase of the dressing depth, it was found that only at a dressing depth more than 2/3 of the average diamond grits diameter, could the wheel be effectively trued by the diamond nib. However, if the dressing depth was chosen to be several times of the average size of the diamond grits, the diamond wheel were not used effectively. Therefore, to improve the service life of the diamond nib and the diamond wheel, the truing and dressing depth was chosen to be 5 μm, which is at the same level as the diameter of the diamond grits. In addition, the grinding spindle speed was selected to be 2,000 RPM to avoid the impact of relative vibration or chattering between the diamond wheel and the truer or dresser, which could result in breakage of

the sharp edge. The SEM image of the edge profile after truing/dressing is shown in Fig. 7, and indicates that the diamond wheel could be well prepared by the proposed method.

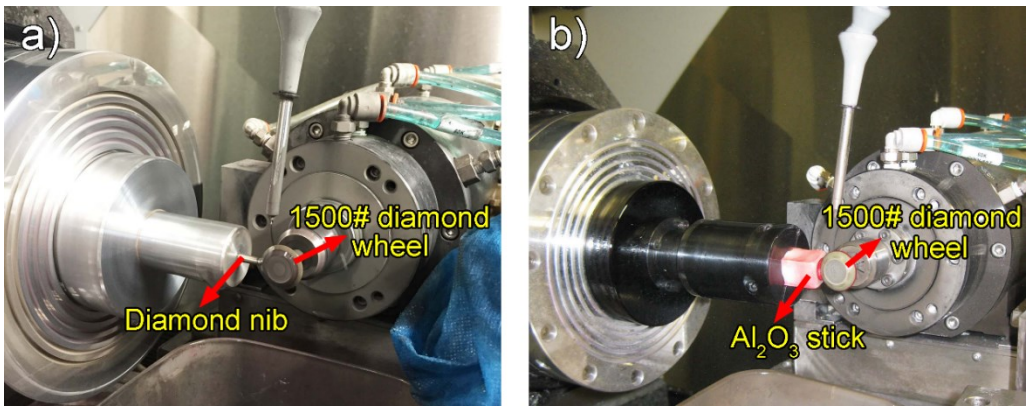

Fig. 6 Truing and dressing of the 1500# diamond wheel: (a) truing by the diamond nib; (b) dressing by the Al_2O_3 stick

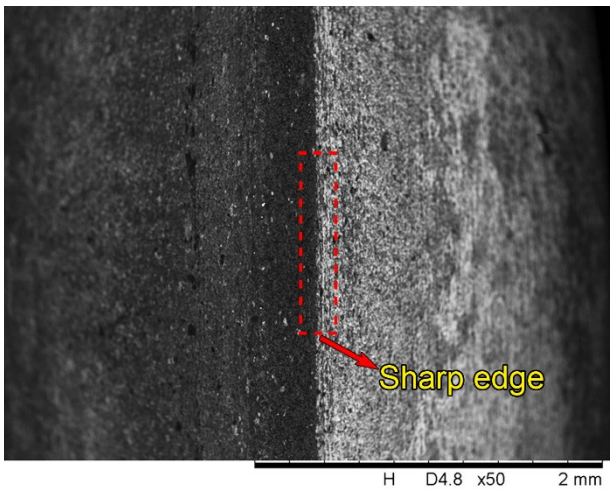

Fig. 7 SEM image of the sharp edge of the diamond wheel after dressing

The obtained sharp edge of the 1500# diamond wheel was measured by the on-machine optical CCD, and is shown in Fig. 8(a). During the ultra-fine grinding stage, the size of the wheel changed after the dressing of the diamond wheel, so several passes of grinding at a cutting depth of 0.5 μm and a feed rate of 0.5 mm/min were firstly performed to adjust the wheel so as to be in contact with the workpiece surface. Then,

after 8 grinding passes at a cutting depth of 0.1 μm and feed rate of 0.1 mm/min, the wheel edge was measured, as shown in Fig. 8(b). Similar to the machining of the hemispherical surfaces in our previous study [17], the rapid loss of the sharp edge appeared during single point diamond grinding of 'water-drop' surface. Therefore, re-dressing of the diamond wheel and compensation of the tool path is of great importance for achieving better surface quality.

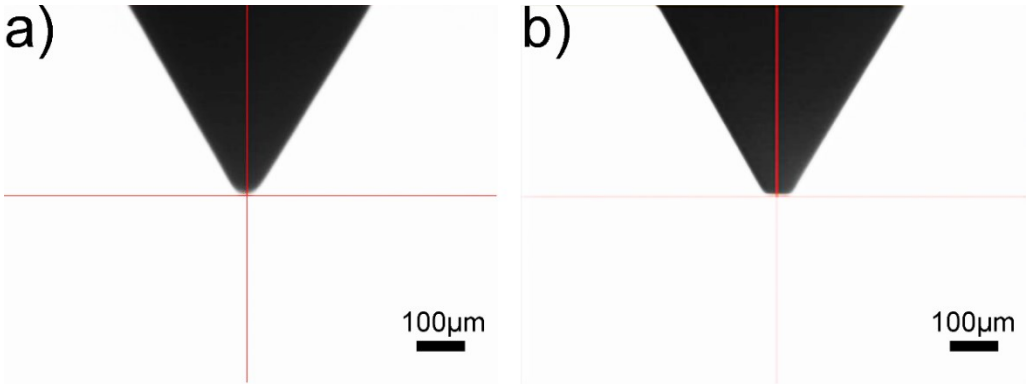

Fig. 8 The measured edge profile of the 1500# diamond wheel after dressing and grinding: (a) after dressing; (b) after grinding

To get a further insight into the diamond wheel wear mechanism, the surface profile and surface morphology of the 1500# diamond wheel is shown in Fig. 9. It can be readily seen that the width of the sharp edge for the diamond wheel after grinding, as shown in Fig. 9(a) and (b), turned to be about 40 μm, which is defined as macro-wheel wear. Besides, the micro wheel wear is involved in diamond grits flattening, grooving and splintering, as shown in Fig. 9(c) and (d). The grinding chips and generated powder (bright region) can also be found on the worn wheel edge, which can result in the diamond wheel blockage.

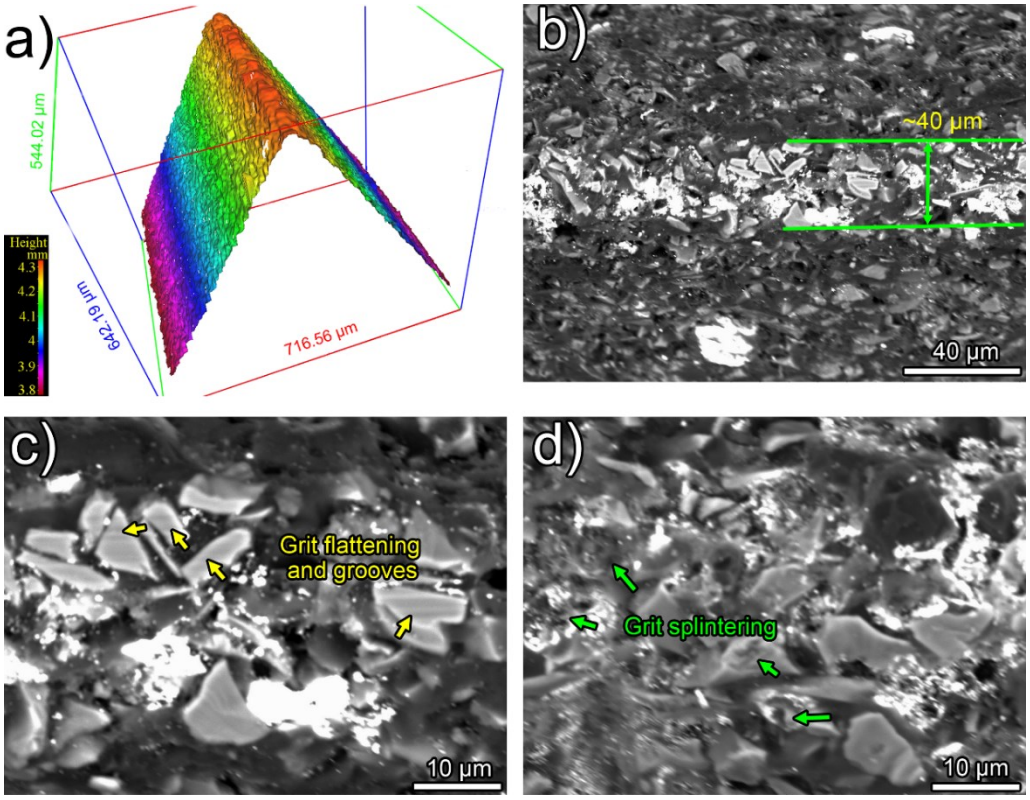

Fig. 9 Surface profile and morphology of the diamond wheel after grinding

4.2 Grinding of 'water-drop' surface

The detailed grinding parameters are listed in Table 3. Fig. 10 shows the form accuracy of the machined 'water-drop' surface measured by the on-machine LVDT probe before and after compensation. It can be seen that the form accuracy was 1.399 µm (*PV*) in a measuring range of 20 mm before the compensation. Actually, the main error of the part mainly appeared around the center at a radial distance of 2 mm, where the removed material volume was the maximum due to the combined effects of vibration and higher overlapping ratio of the grinding points [23, 24]. Specifically, the form error dropped rapidly from the radial distance of 2 mm to the center, and an even linear relation between the measured error data and the radial distance was found, indicated by the blue dotted line, which can be described as follows:

$$z_3 = kx + b \tag{4}$$

To improve the form accuracy of the machined 'water-drop' surface, the linear relation was used to compensate the tool path at the center to improve the form accuracy.

Table 3 Detailed grinding parameters

Grinding	1500# diamond wheel	Diam. 16 mm, resin bonded
	Concentration	100%
	Wheel RPM n_s (rpm)	20,000
	Workpiece RPM n_w (rpm)	120
	Feed rate f (mm/min)	3-0.5-0.1
	Depth of grinding a_e (μm/pass)	2-0.5-0.1
Coolant	CLAIRSOL 350	MQL

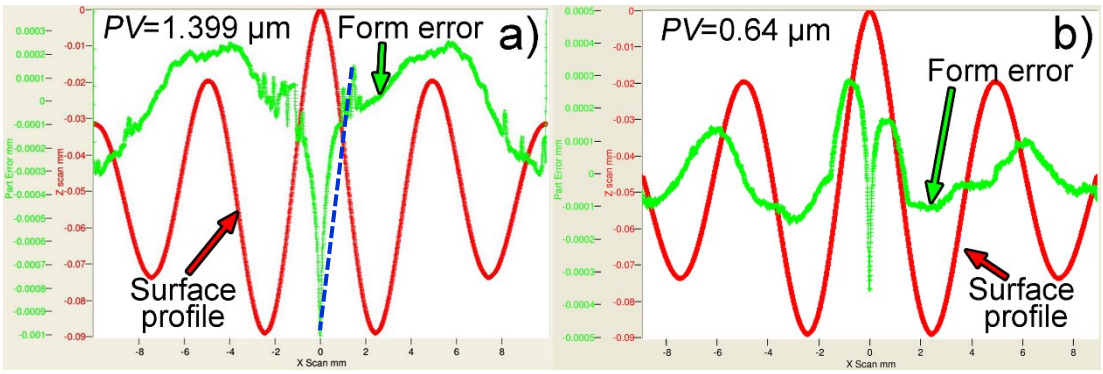

Fig. 10 On-machine measured form accuracy of the machined 'water-drop' surface before and after tool path compensation

In addition, it was found that the form error from the radial distance of 2 mm to the very center is negative, which means that the volume of the removed material is greater than the theoretical volume. Therefore, the tool path should be compensated by adding the absolute data to the tool path at the center, which can be described as:

$$z = z_1 \cdot z_2 + |z_3| = 0.05 \cdot e^{-0.1x} \cdot \cos\frac{4\pi \cdot x}{10} + |kx + b|, \ x \leq 2 \tag{5}$$

As illustrated in Fig. 11, the new tool path indicated that actually the diamond wheel was lifted gradually to reduce the material removal volume at the center region. As shown in Fig. 10(b), it can be readily seen that the form accuracy of the machined 'water-drop' surface after compensation is clearly improved to be 0.64 μm (*PV*), and

the center dent could be significantly alleviated.

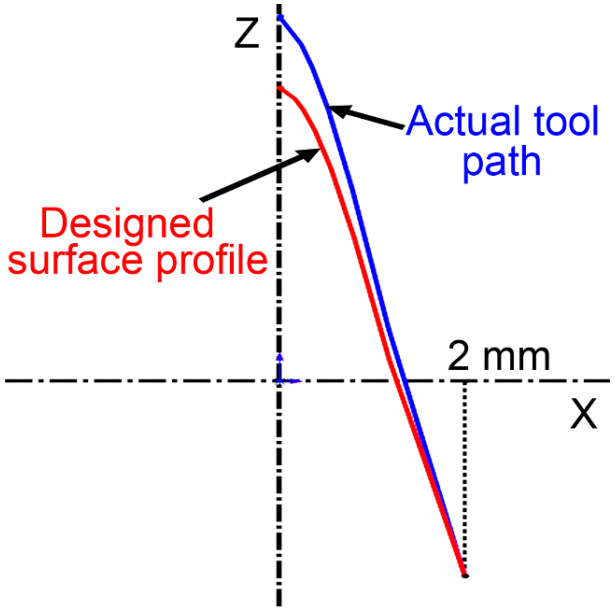

Fig. 11 Illustration of the compensated tool path at center

The cross sectional profile, surface topography and surface roughness obtained by best-fit form removal are shown in Fig. 12. The surface topography after the form removal of the machined "water-drop" surface indicates that the surface roughness (S_a) reaches about 6 nm, lower than 10 nm. Based on previous studies [25-27], the non-uniform surface finish could result from the various material removal rates at different radial positions of a certain workpiece for plane grinding, as the grinding wheel traversed towards the center, where the surface roughness was supposed to drop with decreasing radial distance according to Eqs. (6) and (7) [27, 28].

$$R_a = R_1 \cdot \left(\frac{v_w \cdot h_{\max}}{v_s} \right)^x \tag{6}$$

$$h_{\max} = \left[\frac{4}{Cr} \left(\frac{v_w}{v_s} \right) \left(\frac{a_e}{d_{se}} \right)^{1/2} \right]^{1/2} \tag{7}$$

where R_1 and x are two constants depending on the experiment, v_w is the workpiece speed, v_s is the wheel speed, h_{max} is the max unformed chip thickness, C is the surface

grit density, r is the ratio of chip width to average undeformed chip thickness, a_e is the grinding depth, and d_{se} is the equivalent diameter of the wheel. Nevertheless, it was found that the surface finish for position A (S_a=6 nm) was a little higher than position B (S_a=5 nm). As reported by Chen et al. [29], the effect of h_{max} on the surface finish was marginal compared to the grinding trace spacing (GTS) in grinding tungsten carbide. Here, we propose that not only the trace spacing, but also the density of the grinding trace (DGT) has an influence on the measured surface roughness, and can be expressed as follows:

$$DGT = \frac{N_t}{W_m} \tag{8}$$

where N_t is the total number of grinding grooves and W_m is the imaging width for measurement. In the present work, during the measurement of the surface topography by white light interferometry, the width for imaging is constant at a specific magnification. So the length of the machined curve imaged is higher at a sharper position for data collection by moving the optical lens along the Z direction. Then, the density of the grinding groove is higher after the removal of the form by Gaussian best-fit rule, resulting in a rougher surface, as shown in Fig. 12(d) and (f).

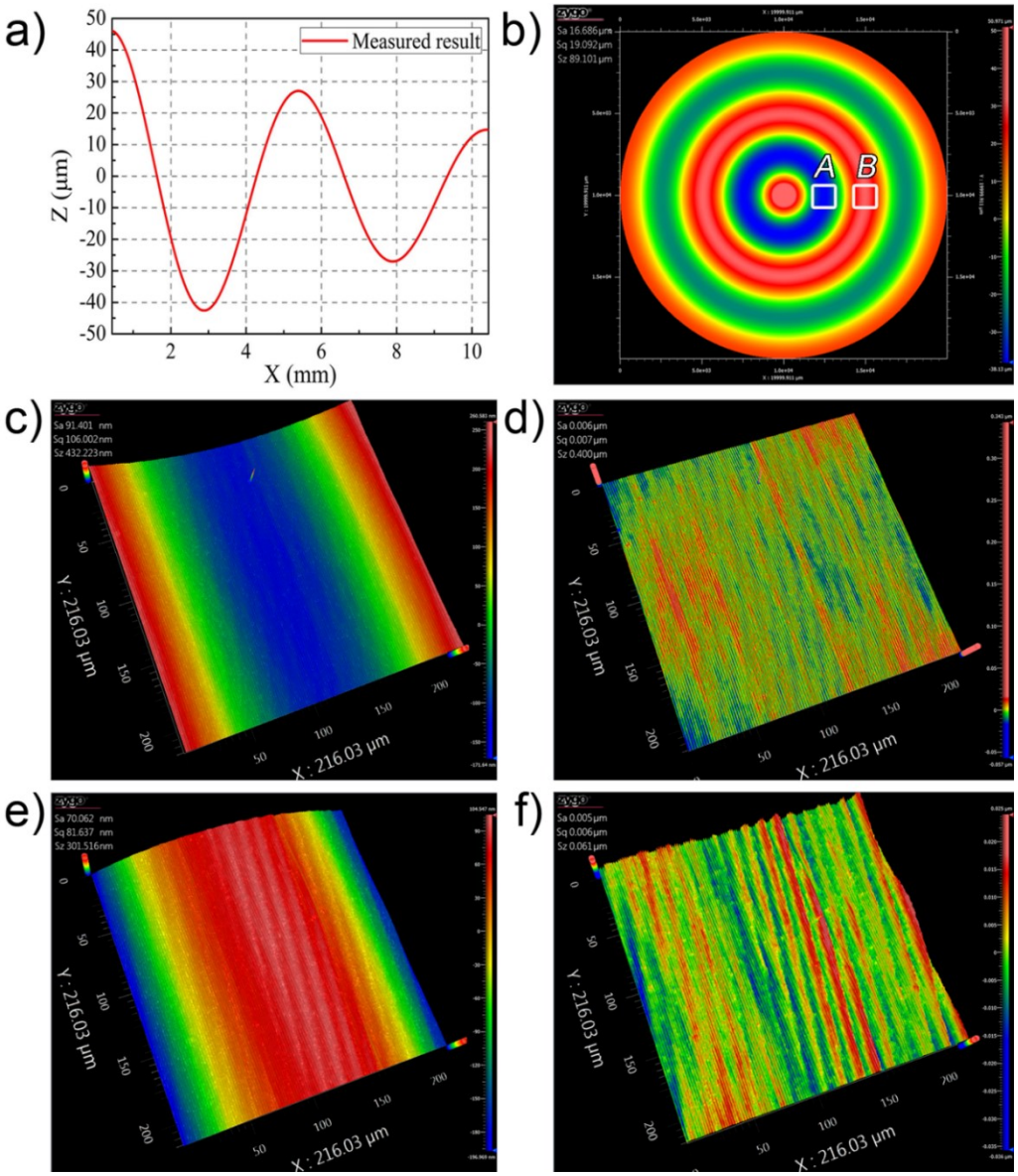

Fig. 12 (a) and (b) Cross-sectional profile and 3D surface topography of the machined 'water-drop' surface; (c) and (d) surface topography and roughness after best-fit form removal of an area 2.5 mm from workpiece center; (e) and (f) surface topography and roughness after best-fit form removal of an area 5 mm from the workpiece center

To get further insight, the surface topography of the machined surface at 5 mm from center was also measured by AFM, as shown in Fig. 13. The result shows that the surface is covered by the grinding grooves of the diamond wheel, and no obvious defects were caused by the grinding process. In addition, the surface roughness further

confirmed that the surface roughness is lower than 10 nm. A mirror surface quality for the machined ‘water-drop’ surface could be achieved, and a photograph of the machined ‘water-drop’ surface is shown in Fig. 14.

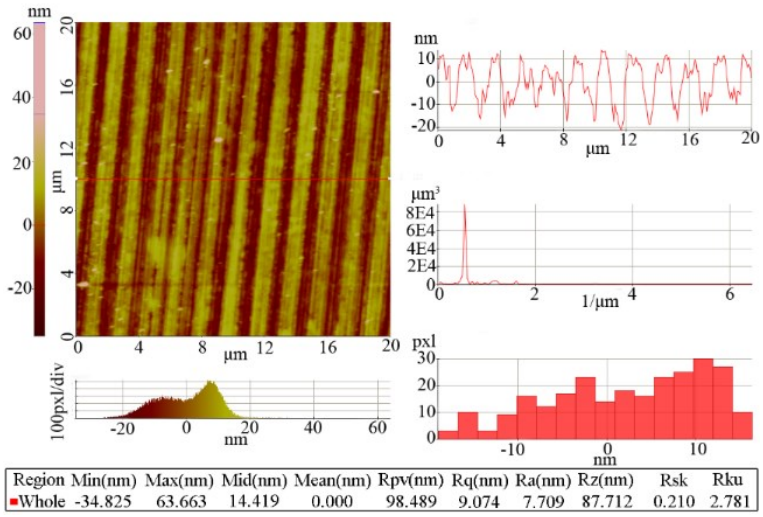

Fig. 13 Surface topography of the machined ‘water-drop’ surface measured by AFM

Fig. 14 Photograph of the machined ‘water-drop’ surface

5. Conclusions

In the present work, the designed ‘water-drop’ surface was precisely machined by single point diamond grinding with the proposed grinding protocol. Before and during the grinding process, the diamond wheel could be well trued by a combination of the diamond nib and Al_2O_3 stick to obtain a sharp grinding edge to prevent interference

between the wheel and the machined surface. However, there was a loss of the sharp edge as the macro wheel wear, and the micro wheel wear involved in grits flattening, grooving and splintering. Moreover, it was found that the main form error for the machined "water-drop" surface appeared at the center of the workpiece, and the proposed linear compensation method from the radial distance of 2 mm contributed to the alleviation of the center dent, with the form accuracy (PV) improved to be 0.64 μm. In addition, a mirror surface quality could be obtained with a surface roughness (S_a) of about 6 nm.

References

[1] F.Z. Fang, X.D. Zhang, A. Weckenmann, G.X. Zhang, C. Evans, Manufacturing and measurement of freeform optics, CIRP Ann. Manuf. Technol. 62 (2013) 823-846.

[2] R. Gläbe, O. Riemer, Diamond machining of micro-optical components and structures, Proceedings of SPIE 7716(2010) 771602.

[3] E. Brinksmeier, Y. Mutlugünes, F. Klocke, J.C. Aurich, P. Shore, H. Ohmori, Ultra-precision grinding, CIRP Ann. Manuf. Technol. 59 (2010) 652-671.

[4] Y.E. Tohme, Grinding aspheric and freeform micro-optical molds, Proc. SPIE 6462 (2007) 64620K.

[5] M. Saeki, T. Kuriyagawa, J. Lee, K. Syoji, Machining of aspherical opto-device utilizing parallel grinding method, The 16th ASPE Annual Meeting 25 (2001) 433-436.

[6] Y. Yamamoto, H. Suzuki, T. Moriwaki, T. Okino, Y. Hijikata, J. Roblee, T.

Miyashita, Development of cross and parallel mode grinding machine for high NA aspherical mold and die, Proceedings of the 13th Annual Meeting of the ASPE (2006) 499-502.

[7] F. Chen, S. Yin, H. Huang, H. Ohmori, Fabrication of small aspheric moulds using single point inclined axis grinding, Precis. Eng. 39 (2015) 107-115.

[8] F. Chen, S. Yin, H. Ohmori, J. Yu, Form error compensation in single-point inclined axis nanogrinding for small aspheric insert, Int. J. Adv. Manuf. Technol. 65 (2013) 433-441.

[9] Y. Zhang, Q. Wu, D. Hu, Research on wear detection of wheel in precision NC curve point grinding, Int. J. Adv. Manuf. Technol. 35 (2008) 994-999.

[10] C. Zhang, R. Rentsch, E. Brinksmeier, Advances in micro ultrasonic assisted lapping of microstructures in hard-brittle materials: a brief review and outlook, Int. J. Mach. Tools Manuf. 45 (2005) 881-890.

[11] G. Spur, S.E. Holl, Ultrasonic assisted grinding of ceramics, J. Mater. Process. Technol. 62 (1996) 287-293.

[12] H. Suzuki, M. Okada, Y. Yamagata, S. Morita, T. Higuchi, Precision grinding of structured ceramic molds by diamond wheel trued with alloy metal, CIRP Ann. - Manuf. Technol. 61 (2012) 283-286.

[13] T. Bletek, F. Klocke, M. Hünten, O. Dambon, Dressing of fine grained diamond grinding wheels for ultraprecision grinding of structured molds in brittle hard materials, Optifab 2013 (2013) 888405-888408.

[14] E. Brinksmeier, O. Riemer, K. Rickens, K. Meiners, Kinematics in ultra-precision

grinding of WC moulds, Int. J. Nanomanuf. 7 (2011) 199-213.

[15] K. Wegener, H.W. Hoffmeister, B. Karpuschewski, F. Kuster, W.C. Hahmann, M. Rabiey, Conditioning and monitoring of grinding wheels, CIRP Ann. - Manuf. Technol. 60 (2011) 757-777.

[16] Q. Zhao, B. Guo, Ultra-precision grinding of optical glasses using mono-layer nickel electroplated coarse-grained diamond wheels. Part 2: Investigation of profile and surface grinding, Precis. Eng. 39 (2015) 67-78.

[17] Q. Zhang, Q. Zhao, S. To, B. Guo, A further study of wheel normal grinding of hemisphere couples on TiC-based cermet, Int. J. Adv. Manuf. Technol. (2016) 1-10.

[18] C. Jiang, Y. Guo, H. Li, Parallel grinding error for a noncoaxial nonaxisymmetric aspheric lens using a fixture with adjustable gradient, Int. J. Adv. Manuf. Technol. 66 (2012) 537-545.

[19] Y. Peng, Y. Dai, C. Song, S. Chen, Error analysis and compensation of line contact spherical grinding with cup-shaped wheel, Int. J. Adv. Manuf. Technol. 83 (2015) 293-299.

[20] H. Huang, W.K. Chen, T. Kuriyagawa, Profile error compensation approaches for parallel nanogrinding of aspherical mould inserts, Int. J. Mach. Tools Manuf. 47 (2007) 2237-2245.

[21] I.S. Jawahir, E. Brinksmeier, R. M'Saoubi, D.K. Aspinwall, J.C. Outeiro, D. Meyer, D. Umbrello, A.D. Jayal, Surface integrity in material removal processes: recent advances, CIRP Ann. - Manuf. Technol. 60 (2011) 603-626.

[22] J.F.G. Oliveira, A.C. Bottene, T.V. França, A novel dressing technique for texturing of ground surfaces, CIRP Ann. - Manuf. Technol. 59 (2010) 361-364.

[23] Q. Zhang, Q. Zhao, S. To, B. Guo, W. Zhai, Diamond wheel wear mechanism and its impact on the surface generation in parallel diamond grinding of RB-SiC/Si, Diam. Relat. Mater. 74 (2017) 16-23.

[24] S.J. Zhang, S. To, G.Q. Zhang, Z.W. Zhu, A review of machine-tool vibration and its influence upon surface generation in ultra-precision machining, Int. J. Mach. Tools Manuf. 91 (2015) 34-42.

[25] Q. Zhang, S. To, Q. Zhao, B. Guo, Surface damage mechanism of WC/Co and RB-SiC/Si composites under high spindle speed grinding (HSSG), Mater. Des. 92 (2016) 378-386.

[26] L. Ma, Y. Gong, X. Chen, Study on surface roughness model and surface forming mechanism of ceramics in quick point grinding, Int. J. Mach. Tools Manuf. 77 (2014) 82-92.

[27] R. Snoeys, J. Peters, A. Decneut, The significance of chip thickness in grinding, Ann. CIRP 23 (1974) 227-237.

[28] S. Malkin, C. Guo, Grinding technology: theory and applications of machining with abrasives, Industrial Press, New York, 2008.

[29] W.K. Chen, T. Kuriyagawa, H. Huang, N. Yosihara, Machining of micro aspherical mould inserts, Precis. Eng. 29 (2005) 315-323.